Location-Based Timing Advance Estimation for 5G Integrated LEO Satellite Communications

Tingting Chen*†, Wenjin Wang*†, Rui Ding‡, Gonzalo Seco-Granados§, Li You*†, and Xiqi Gao*†
*National Mobile Communications Research Laboratory, Southeast University, Nanjing 210096, China
†Purple Mountain Laboratories, Nanjing 211100, China
‡Institute of Telecommunication Satellite, China Academy of Space Technology, Beijing 100094, China
§Telecommunications and Systems Engineering Department, Universitat Autònoma de Barcelona, Barcelona 08193, Spain
Email: {ttchen, wangwj, liyou, xqgao}@seu.edu.cn, greatdn@qq.com, gonzalo.seco@uab.es

GLOBECOM 2020 - 2020 IEEE Global Communications Conference | 978-1-7281-8298-8/20/$31.00 ©2020 IEEE | DOI: 10.1109/GLOBECOM42002.2020.9322428

***Abstract*—Integrated satellite-terrestrial communications networks aim to exploit both the satellite and the ground mobile communications and thus provide genuine ubiquitous coverage. For 5G integrated low earth orbit (LEO) satellite communication (SatCom) systems, the timing advance (TA) is required to be estimated in the initial random access procedure of communications in order to facilitate the uplink frame alignment among different users. However, due to the inherent characteristics of LEO SatCom systems, the existing 5G terrestrial uplink TA scheme is not applicable in the satellite networks. In this paper, we investigate location-based TA estimation for 5G integrated LEO SatCom systems. We propose to take the time difference of arrival (TDOA) and frequency difference of arrival (FDOA) measurements obtained in the downlink timing and frequency synchronization phase for geographical location estimation, which are made from the satellite at different time instants. The location estimation is then formulated as a quadratic optimization problem. We propose an approximation method based on iteratively performing a linearization procedure on the quadratic equality constraints to solve this problem. Numerical results show that the proposed method can effectively assure uplink frame alignment among different users in typical LEO SatCom systems.**

I. Introduction

Recently, with the standardization of the 5G new radio (NR) communication systems and the ongoing resurgence of satellite communications (SatCom), the integration of satellite and terrestrial 5G networks is considered as a promising approach for future mobile communications [1], [2]. Due to the wide-area service coverage capabilities, SatCom networks are expected to foster the roll out 5G services in un-served areas that cannot be covered by terrestrial 5G networks [3]–[7]. Several key impacts in 5G NR protocols/architecture have been identified to provide support for non-terrestrial networks [8]. One of which is the adaptability of the existing 5G uplinking timing advance (TA) method in low earth orbit (LEO) SatCom.

To ensure the uplink intra-cell orthogonality, 5G NR requires that the signals transmitted from different users within the same subframe arrive approximately in a time-aligned manner when reaching the base station (BS), i.e., the BS can receive the uplink frames within the range of one cyclic prefix (CP) [9]. To this end, 5G NR employs an uplink TA scheme during the random access procedure to avoid timing misalignment interference, particularly in the terrestrial networks. However, in a typical LEO SatCom system, the differential time delay will be significantly larger than that of the terrestrial networks. Moreover, the propagation delay in a satellite-to-ground link varies dynamically due to the fast movement of the LEO satellite. Hence, due to these significant differences between the LEO SatCom system and terrestrial wireless one, the existing 5G terrestrial uplink TA scheme is no longer applicable in the LEO SatCom networks.

The TA estimation for random access in non-terrestrial networks (NTN) has been investigated during the past few years. Recent 3rd generation partnership project (3GPP) studies have identified that location information of user equipment (UE) is beneficial for uplink TA estimation [3]. Some proposals also consider several physical random access channel (PRACH) formats for long-distance transmissions, such as the use of long sequences (length = 839) for both FR1 (450 MHz-6 GHz) and FR2 (24.25 GHz-52.6 GHz) operating bands, more repetition or multiple sequence transmissions [10], [11]. For SatCom systems with large Doppler shifts and oscillator uncertainties, symmetric Zadoff-Chu (ZC) sequences have been adopted to estimate TA [12]. In [13], a two-step time delay difference estimation was presented for SatCom systems, which first divides a beam cell into some layered small sub-areas and then two types of PRACH preamble burst formats are transmitted. TA estimation based on the correlation between a ZC sequence and its conjugate replica has been used in [14]. Compared with sending TA commands from the satellite to the UE, signaling overhead can be significantly reduced if the TA value can be estimated directly at the UE side. However, to the best of our knowledge, most previous works on TA estimation

This work was supported in part by the National Key R&D Program of China under Grant 2019YFB1803102, the National Natural Science Foundation of China under Grants 61761136016, 61801114, and 61631018, the Jiangsu Province Basic Research Project under Grant SBK2019050020, the Natural Science Foundation of Jiangsu Province under Grant BK20170688, and the Fundamental Research Funds for the Central Universities. G. Seco-Granados is partially funded by the ICREA Academia programme and by the Spanish Ministry of Science, Innovation and Universities under project TEC2017-89925-R.

978-1-7281-8298-8/20/$31.00 ©2020 IEEE

for SatCom systems were carried out at the satellite side in uplink while little efforts focus on the investigation of TA estimation at the UE side with the utilization of 5G downlink synchronization signals.

In this paper, we propose a novel UE location information-assisted approach for uplink TA estimation in 5G integrated LEO SatCom. Utilizing the 5G downlink primary synchronization signals (PSS) and the CP structure of orthogonal frequency division multiplexing (OFDM), UEs can acquire the timing and frequency offset estimates in the downlink timing-frequency synchronization phase, which can then be transformed into time difference of arrival (TDOA) and frequency difference of arrival (FDOA) measurements [15]. With these measurements, we formulate the equality-constrained optimization problem and propose an iterative constrained weighted least squares (CWLS) method to solve it, then the value of uplink TA can be calculated at the UE side.

II. System Model

A. Timing Advance in 5G Integrated LEO SatCom

In the development of 5G integrated SatCom, most existing works focused on the air interface design of the satellite module to maximize utilization of the technology commonalities with the terrestrial systems, so as to reduce the implementation costs and simplify the interactive procedures. For example, as the 5G NR basic waveform, CP Orthogonal Frequency Division Multiplexing Access (CP-OFDMA) requires that the signals transmitted from different UEs are time-aligned when reaching the BS to keep the uplink intra-cell orthogonality. To this end, 5G NR adopts a scheme for TA during the random access procedure, where the BS first estimates the uplink TA for the UE through the PRACH preamble and then sends the adjustment information to the UE by the random access response (RAR) message [9]. The UE further adjusts its uplink transmission time based on the received TA values combined with the acquired downlink timing synchronization information.

However, such a scheme is designed specifically for the terrestrial networks and may not be applicable to the satellite-to-ground environment. For example, the cell coverage is limited by the CP length of PRACH preambles. The current 5G NR PRACH preambles with $L_{RA} = 839$ formats allow the cell coverage varying from 15 km to 102 km, which may be much smaller than the cell coverage of LEO satellites, even for a single beam coverage [16]. In addition, large variation of the round-trip delay in satellite-to-ground communications within a cell/beam would limit the availability of cyclic shift (CS) multiplexing as well, resulting in smaller cell reuse factor of preamble sequences. On the other hand, the maximum value of the TA command in the RAR message defined in 5G NR may be smaller than the round-trip delay of a LEO satellite-to-ground link [3].

In addition, due to the high-speed motion of the LEO satellite, the satellite-to-ground link usually exhibits a varying propagation delay. As this propagation delay between the UE and satellite is very large, the TA command sent by the satellite is outdated by the time the UE receives it [17]. Hence, to account for this expected TA inaccuracy, an additional adjustment procedure is needed to update the original TA command, as shown in Fig. 1.

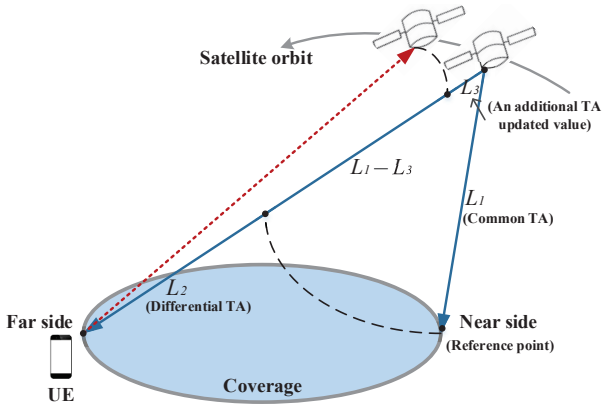

Fig. 1. Illustration of cell/beam coverage of NTN.

In view of these challenges, 3GPP has agreed that several options can be considered to support TA adjustment in random access procedure for NTN. Firstly, when UE positioning capabilities, e.g., GNSS positioning, are enabled at the UE side, they can be used to enhance the TA estimation at the UE side and minimize the amount of signaling required, especially in LEO SatCom systems. Moreover, as indicated by Fig. 1, the total TA can be divided into beam/cell specific common TA L_1 and user-specific differential TA L_2, where the former is used to compensate for the round-trip delay at a reference point within the cell/beam, e.g., the nearest point to the satellite, and the latter is used to represent the difference between the common TA and the actual TA for a specific user [16]. Note that the common TA can be obtained by UEs via broadcast information from the satellite and then only the differential TA should be responded in the RAR message.

B. Location Based Timing Advance Estimation

As the GNSS service may not always be available for UEs, we investigate how a UE can get a rough user-specific TA in 5G integrated LEO SatCom using only downlink signals. In 5G NR, the downlink synchronization signal block (SSB) is introduced, consisting of the primary and secondary synchronization signals. The UE can acquire timing and frequency synchronization within a cell and the physical layer Cell ID through the detection of SSB. In the following, we first introduce the 5G downlink synchronization signals received at the UE side.

Consider K OFDM symbols in one frame. Denote the number of subcarriers and length of CP as N and N_g, respectively. Then the received signal corresponding to the k-th OFDM symbol $s_k(n), k = 1, 2, ..., K, n = 0, 1, ..., N + N_g - 1$ can be given by [15]

$$r_k(n) = e^{j2\pi n\varepsilon/N} \sum_{l=0}^{L-1} h(l) s_k(n - \theta - l) + z(n), \quad (1)$$

where θ denotes the integer-valued symbol timing offset (normalized by the sampling interval) and ε denotes the normalized carrier frequency offset (CFO) with respect to the subcarrier spacing. In addition, $h(l)$, $l = 0, 1, ..., L-1$ denotes the impulse response of a multipath channel with L uncorrelated taps, and $z(n)$ is the additive white Gaussian noise with zero mean and variance σ_z^2.

By using the maximum log-likelihood criterion, discrete prolate spheroidal sequences (DPSS), and the CP structure of OFDM, the timing and frequency offset estimation algorithms in [15] can achieve near optimal performance, i.e., accurate estimation of parameters θ and ε based on the observation $r_k(n)$ at the receiver is available. Let $\widetilde{\theta}_i$ denote the integer-valued normalized symbol timing offset estimation of the i-th SSB with respect to the sampling interval and $\widetilde{\varepsilon}_i$ denote the normalized CFO estimation of the i-th SSB with respect to the subcarrier spacing, $i = 1, 2, ..., M$, where M denotes the total number of downlink SSBs. Consider the initial synchronization timing offset $\widetilde{\theta}_1$ and CFO $\widetilde{\varepsilon}_1$ as the reference, then the estimated TDOA $\widetilde{t}_{i,1}$ and FDOA $\widetilde{f}_{i,1}$, $i = 2, 3, ..., M$ between SSB i and SSB 1 are given by

$$\widetilde{t}_{i,1} = (\widetilde{\theta}_i - \widetilde{\theta}_1)T_s, \quad \widetilde{f}_{i,1} = (\widetilde{\varepsilon}_i - \widetilde{\varepsilon}_1)\Delta f, \tag{2}$$

respectively, where T_s and Δf represent the sampling interval and subcarrier spacing, respectively. Note that TDOA noise $\Delta t_{i,1}$ and FDOA noise $\Delta f_{i,1}$ caused by estimation error of the timing offset and CFO can be written as

$$\widetilde{t}_{i,1} = t_{i,1} + \Delta t_{i,1}, \quad \widetilde{f}_{i,1} = f_{i,1} + \Delta f_{i,1}, \tag{3}$$

where $t_{i,1}$ and $f_{i,1}$ denote the noise-free values of TDOA and FDOA, respectively.

Hence, based on the timing and CFO estimation algorithm with 5G downlink synchronization signals, we can obtain noisy measurements of TDOA and FDOA for geographical location acquisition. Assume that the satellite broadcasts ephemeris periodically, then location information of the UE and satellite is available. Thus, the propagation delay between UE and the satellite can be estimated at the UE side. The UE can then adjust the timing of its uplink transmissions based on the delay estimates. Fig. 2 shows the random access procedure with location-based TA estimation for 5G integrated LEO SatCom. The TA estimation for random access for the 5G integrated LEO SatCom is therefore transformed into the location estimation of the UE with the utilization of downlink synchronization signals. The next section further gives the location estimation algorithms.

III. Location Estimation Algorithms with Downlink Synchronization Signals

A. Problem Formulation

With the relationship between timing/frequency offset estimation and TDOA/FDOA measurements in (2), UE location estimates with the downlink synchronization signals is converted into the geolocation with joint TDOA and FDOA measurements. In this part, we first relate the TDOA and FDOA measurements to the unknown UE location.

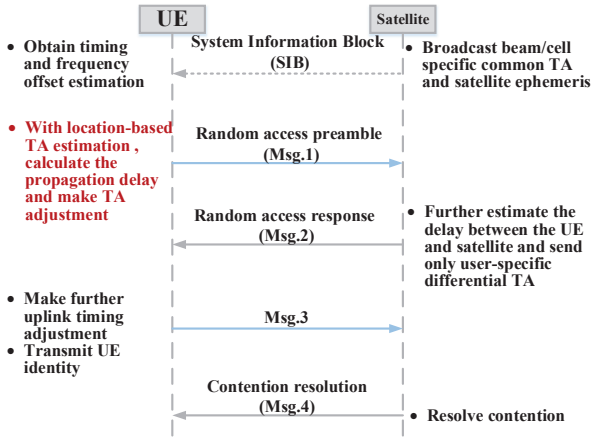

Fig. 2. The random access procedure with location-based TA estimation.

Consider a single LEO satellite with a UE located on the surface of the earth in the Earth Centered Earth Fixed (ECEF) coordinate system, which is aligned with the equatorial plane and the Greenwich meridian [18]. The position and velocity vector of the UE in ECEF are denoted by $\mathbf{p} = [x, y, z]^T$ and $\dot{\mathbf{p}} = [\dot{x}, \dot{y}, \dot{z}]^T$, respectively. The satellite locations $\mathbf{s}_i = [x_i, y_i, z_i]^T$ and velocities $\dot{\mathbf{s}}_i = [\dot{x}_i, \dot{y}_i, \dot{z}_i]^T$ when at the transmit instant of the i-th SSB within the timing-window[1], $i = 1, 2, ..., M$ are assumed to be known thanks to the broadcast satellite ephemeris.

Let d_i, $i = 1, 2, ..., M$ represent the distance between the satellite and the UE corresponding to the i-th downlink SSB given by

$$d_i = \sqrt{(x_i - x)^2 + (y_i - y)^2 + (z_i - z)^2}. \tag{4}$$

Then the range difference of arrival between the i-th and the first SSB related to the TDOAs is given by

$$d_{i,1} = d_i - d_1 = ct_{i,1}, \quad i = 2, 3, ..., M, \tag{5}$$

where c is the speed of light. Taking derivative of (5) with respect to time, we can obtain the range rate differences [19], which are denoted as $\dot{d}_{i,1}$ given by

$$\dot{d}_{i,1} = c\dot{t}_{i,1} = \dot{d}_i - \dot{d}_1, \quad i = 2, 3, ..., M, \tag{6}$$

where $\dot{t}_{i,1}$ and $\dot{d}_i$ denote the rate of change of $t_{i,1}$ and d_i, respectively. From the derivative of (4) with respect to time, $\dot{d}_i$ can be further described as

$$\dot{d}_i = \frac{(\mathbf{s}_i - \mathbf{p})^T(\dot{\mathbf{s}}_i - \dot{\mathbf{p}})}{d_i}. \tag{7}$$

$\dot{t}_{i,1}$ in (6) can be derived from the FDOAs written as [19]

$$f_{i,1} = f_c\dot{t}_{i,1}, \tag{8}$$

where f_c denotes the carrier frequency.

[1]Note that the timing-window refers to the product of the ephemeris broadcasting interval and $(M-1)$, and the ephemeris broadcasting interval is equal to the time interval between two adjacent SSBs.

Taking into account the influence of noises caused by estimation errors of timing and frequency offsets, we define $\widetilde{d}_{i,1}$ and $\widetilde{\dot{d}}_{i,1}$ as the measured value of range and range rate differences, respectively. They can be derived from noisy measurements of TDOA and FDOA sequences and satisfy

$$\widetilde{d}_{i,1} = d_{i,1} + c\Delta t_{i,1}, \quad \widetilde{\dot{d}}_{i,1} = \dot{d}_{i,1} + c\Delta \dot{t}_{i,1}, \tag{9}$$

where $\Delta \dot{t}_{i,1} = \Delta f_{i,1}/f_c$ is equivalent to FDOA noise. Let $\mathbf{n}_t = [c\Delta t_{2,1}, c\Delta t_{3,1}, ..., c\Delta t_{M,1}]^T$ and $\mathbf{n}_f = [c\Delta \dot{t}_{2,1}, c\Delta \dot{t}_{3,1}, ..., c\Delta \dot{t}_{M,1}]^T$ be the vectors of TDOA and FDOA noises, respectively. We assume that they are both zero mean and have covariance matrix as follows,

$$\mathbf{Q}_t = \mathbf{E}[\mathbf{n}_t \mathbf{n}_t^T], \quad \mathbf{Q}_f = \mathbf{E}[\mathbf{n}_f \mathbf{n}_f^T]. \tag{10}$$

Developing the squared term in $d_i^2 = (d_{i,1} + d_1)^2$, and using (4) to span d_i^2 and d_1^2, we can then obtain a set of TDOA equations

$$\begin{aligned} d_{i,1}^2 + 2d_{i,1}d_1 = -2(\mathbf{s}_i - \mathbf{s}_1)^T \mathbf{p} + \mathbf{s}_i^T \mathbf{s}_i - \mathbf{s}_1^T \mathbf{s}_1, \\ i = 2, 3, ..., M. \end{aligned} \tag{11}$$

Further, to make use of FDOAs, we take derivative of (11) with respect to time and obtain

$$\begin{aligned} d_{i,1}\dot{d}_{i,1} + d_{i,1}\dot{d}_1 + \dot{d}_{i,1}d_1 - \mathbf{s}_i^T \dot{\mathbf{s}}_i + \mathbf{s}_1^T \dot{\mathbf{s}}_1 = \\ -(\dot{\mathbf{s}}_i - \dot{\mathbf{s}}_1)^T \mathbf{p} - (\mathbf{s}_i - \mathbf{s}_1)^T \dot{\mathbf{p}}. \end{aligned} \tag{12}$$

Define $\mathbf{u}_1 = [\mathbf{p}^T, \dot{\mathbf{p}}^T, d_1, \dot{d}_1]^T$. Note that $d_{i,1} = \widetilde{d}_{i,1} - c\Delta t_{i,1}$, $\dot{d}_{i,1} = \widetilde{\dot{d}}_{i,1} - c\Delta \dot{t}_{i,1}$, then the set of equations (11) and (12) becomes

$$\mathbf{h}_1 = \mathbf{G}\mathbf{u}_1 + \boldsymbol{\epsilon}, \tag{13}$$

where

$$\mathbf{h}_1 = \begin{bmatrix} \widetilde{d}_{2,1}^2 - \mathbf{s}_2^T \mathbf{s}_2 + \mathbf{s}_1^T \mathbf{s}_1 \\ \widetilde{d}_{3,1}^2 - \mathbf{s}_3^T \mathbf{s}_3 + \mathbf{s}_1^T \mathbf{s}_1 \\ \vdots \\ \widetilde{d}_{M,1}^2 - \mathbf{s}_M^T \mathbf{s}_M + \mathbf{s}_1^T \mathbf{s}_1 \\ 2\widetilde{d}_{2,1}\widetilde{\dot{d}}_{2,1} - 2\mathbf{s}_2^T \dot{\mathbf{s}}_2 + 2\mathbf{s}_1^T \dot{\mathbf{s}}_1 \\ 2\widetilde{d}_{3,1}\widetilde{\dot{d}}_{3,1} - 2\mathbf{s}_3^T \dot{\mathbf{s}}_3 + 2\mathbf{s}_1^T \dot{\mathbf{s}}_1 \\ \vdots \\ 2\widetilde{d}_{M,1}\widetilde{\dot{d}}_{M,1} - 2\mathbf{s}_M^T \dot{\mathbf{s}}_M + 2\mathbf{s}_1^T \dot{\mathbf{s}}_1 \end{bmatrix}, \tag{14}$$

$$\mathbf{G} = -2 \begin{bmatrix} \mathbf{s}_2^T - \mathbf{s}_1^T & \mathbf{0}_{1\times 3} & \widetilde{d}_{2,1} & 0 \\ \mathbf{s}_3^T - \mathbf{s}_1^T & \mathbf{0}_{1\times 3} & \widetilde{d}_{3,1} & 0 \\ \vdots & \mathbf{0}_{1\times 3} & \vdots & \vdots \\ \mathbf{s}_M^T - \mathbf{s}_1^T & \mathbf{0}_{1\times 3} & \widetilde{d}_{M,1} & 0 \\ \dot{\mathbf{s}}_2^T - \dot{\mathbf{s}}_1^T & \mathbf{s}_2^T - \mathbf{s}_1^T & \widetilde{\dot{d}}_{2,1} & \widetilde{d}_{2,1} \\ \dot{\mathbf{s}}_3^T - \dot{\mathbf{s}}_1^T & \mathbf{s}_3^T - \mathbf{s}_1^T & \widetilde{\dot{d}}_{3,1} & \widetilde{d}_{3,1} \\ \vdots & \vdots & \vdots & \vdots \\ \dot{\mathbf{s}}_M^T - \dot{\mathbf{s}}_1^T & \mathbf{s}_M^T - \mathbf{s}_1^T & \widetilde{\dot{d}}_{M,1} & \widetilde{d}_{M,1} \end{bmatrix}, \tag{15}$$

and $\boldsymbol{\epsilon}$ is the error vector derived from (11) and (12). By ignoring the second order error term, $\boldsymbol{\epsilon}$ becomes a Gaussian random vector with covariance matrix given by

$$\boldsymbol{\Psi} = \begin{bmatrix} \mathbf{B} & \mathbf{0} \\ \dot{\mathbf{B}} & \mathbf{B} \end{bmatrix} \begin{bmatrix} \mathbf{Q}_t & \mathbf{0} \\ \mathbf{0} & \mathbf{Q}_f \end{bmatrix} \begin{bmatrix} \mathbf{B} & \dot{\mathbf{B}} \\ \mathbf{0} & \mathbf{B} \end{bmatrix}, \tag{16}$$

where

$$\mathbf{B} = 2\mathrm{diag}\{d_2, d_3, ..., d_M\}, \tag{17}$$

$$\dot{\mathbf{B}} = 2\mathrm{diag}\{\dot{d}_2, \dot{d}_3, ..., \dot{d}_M\}. \tag{18}$$

Consider that the elements of $\mathbf{u}_1$ are statistically independent, then the maximum-likelihood estimation of $\mathbf{u}_1$ can be written as

$$\hat{\mathbf{u}}_1 = \arg\min_{\mathbf{u}_1} \ \{(\mathbf{h}_1 - \mathbf{G}\mathbf{u}_1)^T \boldsymbol{\Psi}^{-1} (\mathbf{h}_1 - \mathbf{G}\mathbf{u}_1)\}. \tag{19}$$

Weighting matrix $\boldsymbol{\Psi}$ is unknown in practice as $\mathbf{B}$ and $\dot{\mathbf{B}}$ contain the accurate satellite-UE distance and its rate of change, respectively. We propose to solve this problem through a further approximation, which considers two typical cases. In the first case of short-time random access procedure, $d_i (i = 1, ..., M)$ is close to each other. Supposing they all approach d^0, then $\mathbf{B} \approx 2d^0\mathbf{I}$ is satisfied, where $\mathbf{I}$ is an identity matrix of size $M-1$. Correspondingly, $\dot{\mathbf{B}} \approx \mathbf{0}$ is also satisfied. Since scaling $\boldsymbol{\Psi}$ does not affect the solution to problem (19), we substitute $\mathbf{I}$ for $\mathbf{B}$ to simplify the weighting matrix. In the other case of initial access for the search of the UE location, since the observation window of the satellite might be much larger, we take the initial values of $\mathbf{B}$ and $\dot{\mathbf{B}}$ as $\mathbf{I}$ and $\mathbf{0}$, respectively, and then iteratively update the weighting matrix with the latest estimation results.

In the solution of problem (19), the correlations among the elements of $\mathbf{u}_1$ are not considered. However, they are related to each other in practice. In the following, we aim to exploit this relationship to provide an improved estimate. Firstly, consider a non-spherical earth model [18] and that the UE is located on the surface of the earth, then the UE location $\mathbf{p}$ satisfies the following equation

$$\frac{x^2}{(R_a)^2} + \frac{y^2}{(R_a)^2} + \frac{z^2}{(R_b)^2} - 1 = 0, \tag{20}$$

where R_a and R_b denote the semi-major and semi-minor axes of the earth, respectively. In addition, the elements of $\mathbf{u}_1$ are also related by (4) and (7) at $i = 1$. With these constraints, the above TDOA/FDOA based location estimation problem in (19) can be reformulated as

$$\begin{aligned} \underset{\mathbf{u}_2}{\text{minimize}} \quad & g(\mathbf{u}_2) = (\mathbf{h}_2 - \mathbf{G}\mathbf{u}_2)^T \boldsymbol{\Psi}^{-1} (\mathbf{h}_2 - \mathbf{G}\mathbf{u}_2), \\ \text{subject to} \quad & c_1(\mathbf{u}_2) = \mathbf{u}_2^T \mathbf{C}_1 \mathbf{u}_2 + 2\mathbf{q}^T \mathbf{u}_2 - \rho = 0, \\ & c_2(\mathbf{u}_2) = \mathbf{u}_2^T \mathbf{C}_2 \mathbf{u}_2 = 0, \\ & c_3(\mathbf{u}_2) = \mathbf{u}_2^T \mathbf{C}_3 \mathbf{u}_2 = 0, \end{aligned} \tag{21}$$

where

$$\mathbf{u}_2 = \mathbf{u}_1 - \widetilde{\mathbf{r}}_1, \tag{22a}$$

$$\widetilde{\mathbf{r}}_1 = (\mathbf{s}_1^T, \dot{\mathbf{s}}_1^T, 0, 0)^T, \tag{22b}$$

$$\mathbf{h}_2 = \mathbf{h}_1 - \mathbf{G}\widetilde{\mathbf{r}}_1, \tag{22c}$$

$$\mathbf{q} = \mathbf{C}_1\widetilde{\mathbf{r}}_1, \tag{22d}$$

$$\rho = 1 - \widetilde{\mathbf{r}}_1^T\mathbf{C}_1\widetilde{\mathbf{r}}_1, \tag{22e}$$

$$\mathbf{r} = [\frac{1}{R_a^2}, \frac{1}{R_a^2}, \frac{1}{R_b^2}]^T, \tag{22f}$$

$$\mathbf{C}_1 = \mathrm{diag}[\mathbf{r}^T, 0, 0, 0, 0, 0], \tag{22g}$$

$$\mathbf{C}_2 = \mathrm{diag}[1, 1, 1, 0, 0, 0, -1, 0], \tag{22h}$$

$$\mathbf{C}_3 = \begin{pmatrix} \mathbf{0}_{3\times3} & \mathbf{I}_{3\times3} & \mathbf{0}_{3\times1} & \mathbf{0}_{3\times1} \\ \mathbf{0}_{3\times3} & \mathbf{0}_{3\times3} & \mathbf{0}_{3\times1} & \mathbf{0}_{3\times1} \\ \mathbf{0}_{1\times3} & \mathbf{0}_{1\times3} & 0 & -1 \\ \mathbf{0}_{1\times3} & \mathbf{0}_{1\times3} & 0 & 0 \end{pmatrix}. \tag{22i}$$

B. Iterative CWLS Algorithm

The optimization problem in (21) is a quadraric programming with three quadratic equality constraints. Quadratic penalty method is commonly used in practice to solve the equality-constrained problems because of its simplicity [20], however, it tends to have a high computational complexity since it requires both inner and outer iterations. In the following, we propose an iterative CWLS method to solve the equality-constrained optimization problem.

The method starts from an initial estimate of $\mathbf{u}_2$. Then, we write one of the variables $\mathbf{u}_2$ in $c_i(\mathbf{u}_2), i = 1, 2, 3$ as a combination of the estimated value $\hat{\mathbf{u}}_2$ and the estimated error $\Delta\mathbf{u}_2$. With the estimated value of $\mathbf{u}_2$, we convert the problem in (21) into an approximate quadratic programming with linear equality constraints, which is verified to have a closed-form solution in [21]. Next, we update the linear equality constraints with the latest estimation of $\mathbf{u}_2$ and solve the approximate quadratic programming iteratively. In the following, we give more detailed descriptions of this method.

An initial estimate of $\mathbf{u}_2$ can be calculated by (19) as

$$\hat{\mathbf{u}}_2 = (\mathbf{G}^T\mathbf{\Psi}^{-1}\mathbf{G})^{-1}\mathbf{G}^T\mathbf{\Psi}^{-1}\mathbf{h}_2. \tag{23}$$

Then, the approximate quadratic programming with linear equality constraints based on (21) can be formulated as

$$\begin{aligned} \underset{\mathbf{u}_2}{\text{minimize}} \quad & g(\mathbf{u}_2) = (\mathbf{h}_2 - \mathbf{G}\mathbf{u}_2)^T\mathbf{\Psi}^{-1}(\mathbf{h}_2 - \mathbf{G}\mathbf{u}_2), \\ \text{subject to} \quad & c_1(\mathbf{u}_2) = (\hat{\mathbf{u}}_2^T\mathbf{C}_1 + 2\mathbf{q}^T)\mathbf{u}_2 - \rho = 0, \\ & c_2(\mathbf{u}_2) = \hat{\mathbf{u}}_2^T\mathbf{C}_2\mathbf{u}_2 = 0, \\ & c_3(\mathbf{u}_2) = \hat{\mathbf{u}}_2^T\mathbf{C}_3\mathbf{u}_2 = 0. \end{aligned} \tag{24}$$

The above problem (24) has been proved to possess a closed-form solution [21], which can be expressed as

$$\breve{\mathbf{u}}_2 = (\mathbf{P}_1\mathbf{G}^T\mathbf{\Psi}^{-1}\mathbf{G}\mathbf{P}_1)^{\dagger}(\mathbf{G}^T\mathbf{\Psi}^{-1}\mathbf{h}_2 - \mathbf{G}^T\mathbf{\Psi}^{-1}\mathbf{G}\mathbf{P}_2) + \mathbf{P}_2, \tag{25}$$

where

$$\mathbf{P}_1 = \mathbf{I} - \mathbf{A}^T(\mathbf{A}\mathbf{A}^T)^{-1}\mathbf{A}, \tag{26a}$$

$$\mathbf{P}_2 = \mathbf{A}^T(\mathbf{A}\mathbf{A}^T)^{-1}\mathbf{b}, \tag{26b}$$

$$\mathbf{A} = [(\hat{\mathbf{u}}_2^T\mathbf{C}_1 + 2\mathbf{q}^T); \hat{\mathbf{u}}_2^T\mathbf{C}_2; \hat{\mathbf{u}}_2^T\mathbf{C}_3], \tag{26c}$$

$$\mathbf{b} = [\rho; 0; 0]. \tag{26d}$$

TABLE I
SIMULATION SETUP PARAMETERS

Parameter	Value
Orbital altitude	1070 km
Eccentricity of the orbit	0
Inclination of the orbit	85°
Argument of perigee of the orbit	0
Right ascension of ascending node of the orbit	0
Carrier frequency	2.6 GHz
Half viewing angle of the satellite	57°
Minimum elevation angle of the UE	20°

TABLE II
LOCATION OF THE GROUND TERMINALS

Ground terminal	Location	Elevation angle
Sub-satellite point	(6°N , 0°E)	90°
Pos1	(20°N , 0°E)	22°
Pos2	(6°N , 15°E)	22°

With the estimate of $\mathbf{u}_2$ in (25), the iteratively updated approximate quadratic programming (24) can be closer to the original problem (21). As the CWLS method derives a closed form solution to the approximate problem (24) and only requires to update the $\mathbf{u}_2$ iteratively by (25), the computational complexity of the proposed method can be low.

IV. NUMERICAL RESULTS

The numerical results are provided to evaluate the performance of our proposed CWLS method for estimating the TA in 5G integrated LEO SatCom. Due to the requirements of downlink synchronization defined for NTN UE in [3], the signal-to-noise ratio (SNR) of synchronization in downlink is set to be -6 dB in this simulation. A multipath fading channel with system bandwidth 20 MHz and sampling frequency 30.72 MHz is adopted. The major simulation setup parameters are listed in Table I.

In the simulation part, we first select three representative UE locations in the single-satellite beam coverage area, which are sub-satellite point and two positions (*Pos1* and *Pos2*) at the region edge with lower elevation angles. *Pos1* is in the direction of the sub-satellite trajectory and *Pos2* is in the vertical direction of this trajectory. The detailed locations of these ground terminals are given in Table II. The number of independent runs in each result is 2000.

We first study the shortest possible timing-window with the guaranteed performance of TA estimation. Keeping the ephemeris broadcasting interval = 20 ms, Fig. 3 shows the cumulative probability distribution of TA estimation error of different UEs. We can observe that for a given ephemeris broadcasting interval of 20 ms, the timing-window of 12 s can guarantee that the TA estimation offsets of all uplink frames to fall within the range of one CP.

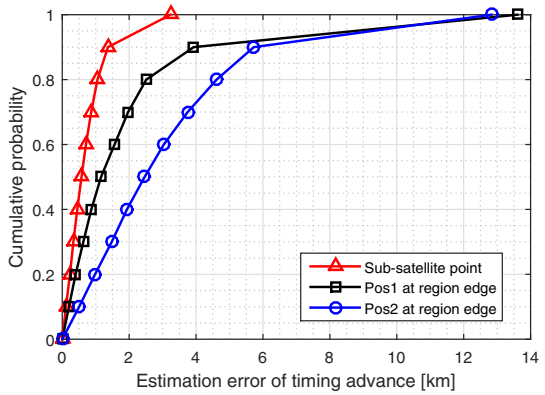

Fig. 3. The cumulative probability distribution of TA estimation error (Ephemeris broadcasting interval: 20 ms; timing-window: 12 s).

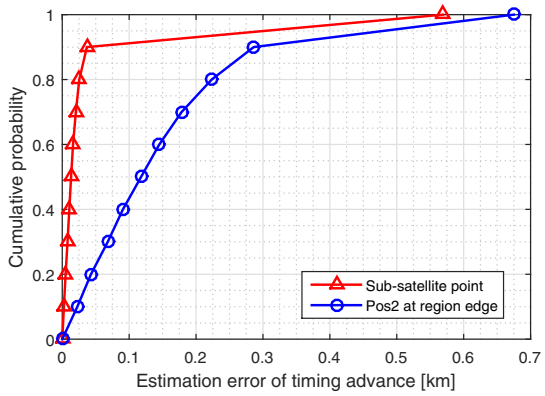

Fig. 4. The cumulative probability distribution of TA estimation error during the whole satellite visibility window (Ephemeris broadcasting interval: 50 s).

Next, we study the largest possible ephemeris broadcasting interval with the guaranteed performance of TA estimation during the whole visibility window of the satellite. Fig. 4 shows the cumulative probability distribution of TA estimation error during the whole visibility window. It can be clearly seen that for the entire satellite visibility window, the ephemeris broadcasting interval can be enlarged to 50 s.

V. Conclusion

In this paper, we proposed a new approach aided by the UE geolocation to perform uplink TA for random access in 5G integrated LEO SatCom with the TDOA and FDOA measurements acquired in the downlink timing and frequency synchronization phase, thus settling the inadaptability of the TA scheme initially designed for 5G NR system in 5G integrated LEO SatCom. We introduced an equality-constrained quadratic optimization problem from the system model and then adopted an iterative CWLS algorithm to solve it. Numerical results showed that the proposed method can effectively achieve uplink frame alignment across UEs in typical LEO SatCom systems.

References

[1] O. Kodheli, A. Guidotti, and A. Vanelli-Coralli, "Integration of satellites in 5G through LEO constellations," in *Proc. IEEE GLOBECOM*, Singapore, 2017, pp. 1–6.

[2] G. Giambene, S. Kota, and P. Pillai, "Satellite-5G integration: A network perspective," *IEEE Netw.*, vol. 32, no. 5, pp. 25–31, Sep./Oct. 2018.

[3] 3GPP TR 38.811 V15.2.0, "3rd Generation Partnership Project; Technical Specification Group Radio Access Network; Study on New Radio (NR) to Support Non Terrestrial Networks (Release 15)," Tech. Rep., Sep. 2019.

[4] A. Kapovits, M. Corici, I. Gheorghe-Pop, A. Gavras, F. Burkhardt, T. Schlichter, and S. Covaci, "Satellite communications integration with terrestrial networks," *China Commun.*, vol. 15, no. 8, pp. 22–38, Aug. 2018.

[5] W. Wang, A. Liu, Q. Zhang, L. You, X. Q. Gao, and G. Zheng, "Robust multigroup multicast transmission for frame-based multi-beam satellite systems," *IEEE Access*, vol. 6, pp. 46 074–46 083, Aug. 2018.

[6] L. You, A. Liu, W. Wang, and X. Q. Gao, "Outage constrained robust multigroup multicast beamforming for multi-beam satellite communication systems," *IEEE Wireless Commun. Lett.*, vol. 8, no. 2, pp. 352–355, Apr. 2019.

[7] L. You, K.-X. Li, J. Wang, X. Q. Gao, X.-G. Xia, and B. Ottersten, "Massive MIMO transmission for LEO satellite communications," *IEEE J. Sel. Areas Commun.*, vol. 38, no. 8, pp. 1851–1865, Aug. 2020.

[8] A. Guidotti, A. Vanelli-Coralli, M. Conti, S. Andrenacci, S. Chatzinotas, N. Maturo, B. Evans, A. Awoseyila, A. Ugolini, T. Foggi, L. Gaudio, N. Alagha, and S. Cioni, "Architectures and key technical challenges for 5G systems and incorporating satellites," *IEEE Trans. Veh. Technol.*, vol. 68, no. 3, pp. 2624–2639, Mar. 2019.

[9] E. Dahlman, S. Parkvall, and J. Sköld, *5G NR: The Next Generation Wireless Access Technology*. Waltham, MA, USA: Academic Press, 2018.

[10] H. Saarnisaari, A. O. Laiyemo, and C. H. M. de Lima, "Random access process analysis of 5G new radio based satellite links," in *Proc. 2019 IEEE 2nd 5GWF*, Dresden, Germany, 2019, pp. 654–658.

[11] L. Zhen, H. Qin, B. Song, R. Ding, X. Du, and M. Guizani, "Random access preamble design and detection for mobile satellite communication systems," *IEEE J. Sel. Areas Commun.*, vol. 36, no. 2, pp. 280–291, Feb. 2018.

[12] G. Cui, Y. He, P. Li, and W. Wang, "Enhanced timing advanced estimation with symmetric Zadoff-Chu sequences for satellite systems," *IEEE Commun. Lett.*, vol. 19, no. 5, pp. 747–750, May 2015.

[13] C. Li, H. Ba, H. Duan, Y. Gao, and J. Wu, "A two-step time delay difference estimation method for initial random access in satellite LTE system," in *Proc. 16th Int. Conf. Adv. Commun. Technol.*, Pyeongchang, South Korea, 2014, pp. 10–13.

[14] Y. He, G. Cui, P. Li, R. Chang, and W. Wang, "Timing advanced estimation algorithm of low complexity based on DFT spectrum analysis for satellite system," *China Commun.*, vol. 12, no. 4, pp. 140–150, Apr. 2015.

[15] W. Wang, Y. Tong, L. Li, A. Lu, L. You, and X. Q. Gao, "Near optimal timing and frequency offset estimation for 5G integrated LEO satellite communication system," *IEEE Access*, vol. 7, pp. 3298–3310, Aug. 2019.

[16] 3GPP R1-1912470, "Uplink timing advance/RACH procedure and initial access for NTN," in *3GPP TSG RAN WG1 Meeting 99*, Reno, USA, Nov. 2019.

[17] 3GPP R1-1910982, "On NTN synchronization, random access, and timing advance," in *3GPP TSG RAN WG1 Meeting 98bis*, Chongqing, China, Oct. 2019.

[18] O. Montenbruck and E. Gill, *Satellite Orbits-Models, Methods, and Applications*. New York, NY, USA: Springer-Verlag, 2000.

[19] K. C. Ho and Y. T. Chan, "Geolocation of a known altitude object from TDOA and FDOA measurements," *IEEE Trans. Aerosp. Electron. Syst.*, vol. 33, no. 3, pp. 770–782, Jul. 1997.

[20] J. Nocedal and S. J. Wright, *Numerical Optimization*, 2nd ed. New York, NY, USA: Springer-Verlag, 2006.

[21] X. M. Qu, L. H. Xie, and W. R. Tan, "Iterative constrained weighted least squares source localization using TDOA and FDOA measurements," *IEEE Trans. Signal Process.*, vol. 65, no. 15, pp. 3990–4003, Aug. 2017.